

Improving the Stability of Supercapacitors at High Voltages and High Temperatures by the Implementation of Ethyl Isopropyl Sulfone as Electrolyte Solvent

Lukas Köps, Fabian Alexander Kreth, Desirée Leistenschneider, Konstantin Schutjajew, Rebecka Gläßner, Martin Oschatz, and Andrea Balducci*

Two of the main weaknesses of modern electric double-layer capacitors are the rather limited ranges of operating voltage and temperature in which these devices do not suffer from the occurrence of irreversible decomposition processes. These parameters are strongly interconnected and lowering the operating voltage when increasing the temperature is unavoidable, so as to protect the electric double-layer capacitor from damage. With the aim to maintain the operating voltage as high as possible at elevated temperatures, in this study, the application of ethyl isopropyl sulfone as an electrolyte solvent for electric double-layer capacitors is presented. It is shown that ethyl isopropyl sulfone-based electrolytes display excellent thermal and electrochemical stability enabling high capacitance retention after floating tests for 500 h at 60 and 80 °C, e.g. 68% at 3.4 V at 60 °C. A possible reason for the above-average stability is that decomposition products of ethyl isopropyl sulfone can deposit on the electrode surface which may act as a passivation layer and prevent further degradation.

1. Introduction

The great efforts to reduce the dependency on fossil fuels and energy of the global society increase the demand for electric energy storage tremendously. Besides batteries and fuel cells, electric double-layer capacitors (EDLCs) are among the most


promising technologies.^[1] EDLCs display high power densities and extremely high lifetime which makes them the technology of choice for a variety of applications requiring a fast and continuous delivery of energy. However, as the energy density of these devices is rather limited (5–8 Wh kg⁻¹), their use is currently limited to applications that require a relatively low amount of energy.^[2] As indicated by several studies, an increase in energy density would lead to a drastic increase in the number of possible applications for EDLCs.^[3] Furthermore, it would enable the use of these devices as replacement for established battery systems in fields where high power is required.^[4] This latter application is particularly interesting because nowadays the use of batteries in high-power applications is typically leading to increased cell degradation and,

consequently, to increased cost due to early system failure. For this reason, in the available electric vehicles, EDLCs are often applied as a support to reduce the load on the main battery system during rapid acceleration and power uptake by regenerative braking. It has been shown that this hybrid energy storage solution results in improved performance while extending the lifetime of the battery system.^[5] Nonetheless, further improvements are urgently needed to extend the battery life even more.

For these reasons, current research focuses on the development of EDLCs with improved energy density. To reach this goal, the electrode capacitance needs to be maximized and, at the same time, the operating voltage of these systems needs to be significantly increased. While commercially available devices are limited to operating voltages of up to 3.0 V, an increase to 3.2 V or more would increase the energy density significantly. The operating voltage of EDLCs is mainly determined by the onset of electrolyte decomposition at the electrode surface.^[6] The state-of-the-art electrolytes consist of solutions containing ammonium-based conducting salt, e.g. tetraethylammonium tetrafluoroborate (TEABF₄), dissolved in acetonitrile (ACN).^[7] These electrolytes display high conductivity but guarantee high stability only if used in devices with a maximum voltage of 3 V.^[8] With the aim to overcome this limitation and realize high-voltage EDLCs, a variety of novel solvents, salts, and ionic liquids have been investigated in the last years.^[9] Although

L. Köps, F. A. Kreth, D. Leistenschneider, K. Schutjajew, R. Gläßner, M. Oschatz, A. Balducci
Institute for Technical Chemistry and Environmental Chemistry
Friedrich-Schiller-University Jena
Philosophenweg 7a, 07743 Jena, Germany
E-mail: andrea.balducci@uni-jena.de

L. Köps, F. A. Kreth, D. Leistenschneider, K. Schutjajew, R. Gläßner, M. Oschatz, A. Balducci
Center for Energy and Environmental Chemistry Jena (CEEC Jena)
Friedrich-Schiller-University Jena
Philosophenweg 7a, 07743 Jena, Germany

 The ORCID identification number(s) for the author(s) of this article can be found under <https://doi.org/10.1002/aenm.202203821>.

© 2022 The Authors. Advanced Energy Materials published by Wiley-VCH GmbH. This is an open access article under the terms of the Creative Commons Attribution-NonCommercial License, which permits use, distribution and reproduction in any medium, provided the original work is properly cited and is not used for commercial purposes.

DOI: 10.1002/aenm.202203821

encouraging results have been obtained, these novel electrolytes have not yet been introduced in commercial devices. Thus, the development of novel electrolytes is currently seen as a key factor for the realization of high-energy EDLCs.

EDLCs utilizing organic electrolytes can operate properly only in a limited range of temperatures. This range is set by the usually low boiling point and high volatility of the organic solvent. At high temperatures, the electrolyte solvent starts to evaporate, which results first of all in poor cell performance due to less liquid solvent molecules and pore blocking by the adsorption of gaseous solvent molecules. Additionally, solvent evaporation leads to a security risk by the internal pressure buildup inside the cell housing and, in the worst case, to a venting event or even the explosion of the cell.^[10] Additionally, increased temperatures accelerate parasitic reactions by providing the necessary activation energy for a given decomposition reaction and enable faster transport of fresh reactants toward the electrode surface and products away from the electrode surface. For this reason, one important aspect to be considered while developing novel electrolytes for EDLCs is the electrochemical and chemical stability at high temperatures.

Among the alternative considered electrolyte solvents, sulfones seem to be promising candidates for the application in high-voltage EDLCs operating at elevated temperatures as shown by Chiba et al.^[11] Ethyl isopropyl sulfone (EiPS), in particular, displays a higher boiling point than common and industrially used solvents like propylene carbonate and acetonitrile, comparable physicochemical properties such as viscosity and dielectric constant, and low reactivity with water, resulting in high electrochemical stability.^[11] Schütter et al. demonstrated the high electrochemical stability of this alternative solvent and were able to show that its use in EDLCs allows the realization of devices with an operating voltage of 3.4 V.^[12] These properties make EiPS an interesting electrolyte solvent for application in high-voltage EDLCs. Nevertheless, further investigation is needed to understand the electrochemical performance of EDLCs based on EiPS at elevated temperatures.

In order to get further insights, the electrochemical behavior of high-voltage EiPS-based EDLCs at different temperatures, ranging from 20 to 80 °C is studied in this work in detail. The decomposition products generated in these devices have been

investigated in detail utilizing post-mortem gas chromatography-mass spectrometry (GC-MS) and X-ray photoelectron spectroscopy (XPS) in order to gain a deeper understanding of the underlying degradation mechanisms. The former technique has been utilized to analyze the degradation products present in the electrolyte, while the latter has been used to analyze those present on the electrode surface.

2. Results and Discussion

In order to understand the behavior of EiPS-based electrolytes, a solution containing this solvent and the state-of-the-art salt TEABF₄ was prepared. As indicated by Chiba et al., EiPS has a limited ability to dissolve salts. For this reason, it is challenging to realize highly concentrated electrolytes utilizing this solvent.^[11] In the case of this study, we investigated the salt TEABF₄ at a concentration of 0.5 M in EiPS. This concentration is the highest achievable with this solvent-salt combination at room temperature. The properties of this alternative electrolyte have been compared to that of the state-of-the-art electrolyte 1 M TEABF₄ in ACN. **Figure 1a** depicts the ionic conductivity of the considered electrolytes in a temperature range of -30–80 °C. As shown, over the whole temperature range, the ACN-based electrolyte displays higher ionic conductivity than the alternative electrolyte based on EiPS. While the ACN-based electrolyte displays a conductivity of 26.1 mS cm⁻¹ at -30 °C, the EiPS-based electrolyte is solid at this temperature due to its melting point of -8 °C.^[11] With increasing temperature, both electrolytes show an increase in ionic conductivity. At 20 °C the conventional electrolyte is displaying a conductivity of 53 mS cm⁻¹, while the EiPS-based electrolyte shows a conductivity of 2.2 mS cm⁻¹. At a temperature of 80 °C, the alternative electrolyte features a conductivity of 8.7 mS cm⁻¹, while the conductivity of the state of the art is 97.3 mS cm⁻¹. Considering the viscosity of the investigated electrolytes shown in **Figure 1b**, the behavior in the same temperature range follows a comparable trend, with improving transport properties at increasing temperatures as indicated by the decreasing viscosity. At a low temperature of -30 °C, 0.5 M TEABF₄ in EiPS displays a viscosity of 129.5 mPa s, while the reference electrolyte shows a significantly lower viscosity of

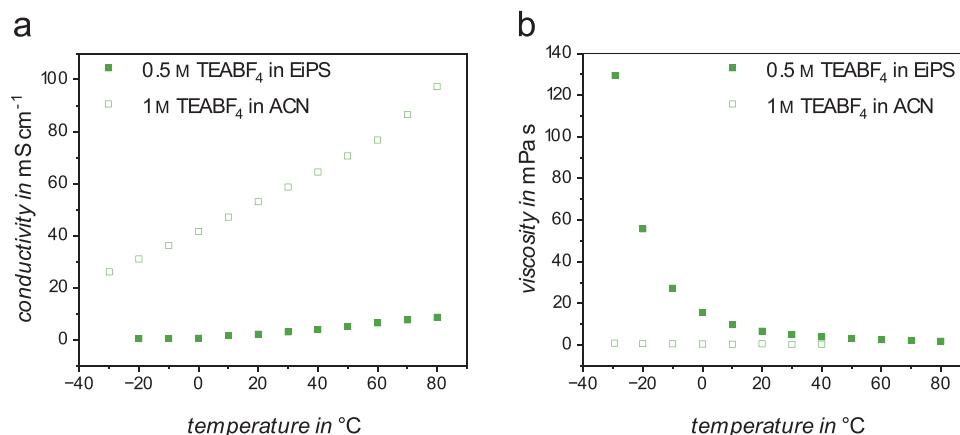


Figure 1. Comparison of a) ionic conductivity and b) viscosity of 0.5 M TEABF₄ in EiPS and 1 M TEABF₄ in ACN in a temperature range between -30 and 80 °C.

0.5 mPa s. When the temperature increases to 20 °C, the difference between the investigated electrolytes becomes smaller with viscosities of 0.2 and 6.7 mPa s featured by the conventional and alternative electrolytes, respectively. At temperatures higher than 40 °C, the ACN evaporates from the open experimental setup of the viscometer resulting in a limited temperature range of measurement, while the EiPS-based electrolyte shows no evaporation at this temperature due to the higher boiling point. At 80 °C, the alternative electrolyte provides a viscosity of 1.8 mPa s.

It is evident that the transport properties of 0.5 M TEABF₄ in EiPS are less favorable than those of the state of the art, but they are comparable to those of other alternative solvents (see Table S1 of the Supporting Information). Furthermore, at high temperatures, where ACN is evaporating, the EiPS is stable and displays conductivity and viscosity values that are suitable for application in EDLCs. This is also evident when the energy and power delivered by EDLCs containing these two electrolytes and working at different temperatures are compared (see Figure S1 of the Supporting Information).

In order to investigate the impact of 0.5 M TEABF₄ in EiPS on the electrochemical performance of EDLCs, floating tests over a time of 500 h at different voltages and different temperatures (20, 60, and 80 °C) were performed. The stability of the investigated devices was compared to that of EDLCs containing 1 M TEABF₄ in ACN tested under similar conditions. The evolution of the corresponding charge–discharge profiles during the float tests is shown in Figure S2 of the Supporting Information. As depicted in Figure 2a, at 20 °C EiPS-based EDLCs display capacitance retention of 90% after 500 h of floating at 3.4 V while they are able to retain 74% after 500 h of floating at 3.6 V. This stability is among the highest reported for lab scale EDLCs tested in these very harsh conditions, and it is higher than that observed for the ACN-based EDLCs, which display capacitance retention of 49% after 500 h floating at 3.4 V.^[8a] When the EDLCs were tested at the same voltage, but at 60 °C, the stability of the EDLCs became significantly different. As shown in Figure 2b, ACN-based EDLCs lose 53% of their initial capacitance after 200 h of floating. This low stability is confirming that the use of the state-of-the-art electrolyte in these operating conditions cannot guarantee sufficient stability. The use of 0.5 M TEABF₄ in EiPS significantly improves the stability of the device. As a matter of fact, as shown, the EiPS-based device is able to retain 68% of its initial capacitance after 500 h of floating at 3.4 V. When the floating test was carried out at 3.2 V, the stability was further improved, and the device retains 75% of its initial capacitance after 500 h of floating. Finally, also the stability of the devices at 80 °C has been investigated. As shown in Figure 2c, when EiPS-based EDLCs are floated at 3.2 V at this high temperature, their stability is very limited, and after 100 h they lose almost all their initial capacitance. However, when the floating voltage is reduced to 3.0 V the stability of the devices increases significantly, and after 500 h of floating the devices are able to retain 62% of their initial capacitance. To the best of our knowledge, this is the highest stability reported so far for an EDLC operating at 80 °C with a cell voltage of 3.0 V. These results are clearly indicating that the use of 0.5 M TEABF₄ in EiPS makes the realization of high-voltage EDLCs that display

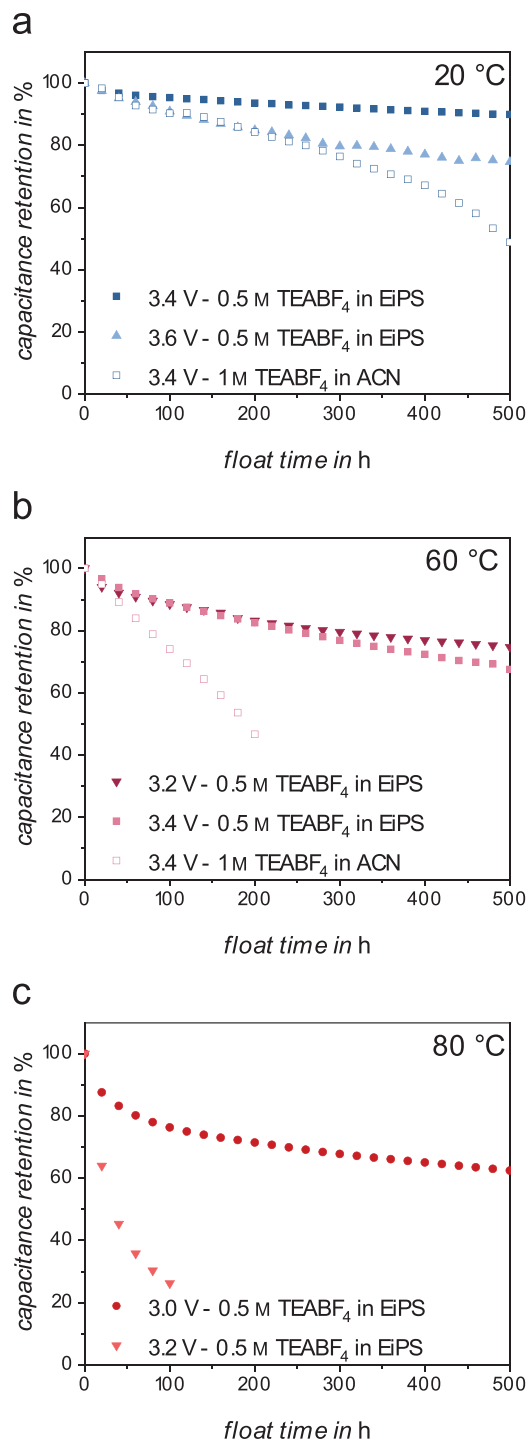


Figure 2. Influence of different voltages on the floating stability of 0.5 M TEABF₄ in EiPS and 1 M TEABF₄ in ACN at 20 °C a), 60 °C b), and 80 °C c).

excellent capacitance retention up to 80 °C possible. For this reason, this electrolyte can be considered a very interesting alternative to the state of the art, especially for high-temperature applications.

In order to understand the direct impact of the temperature on the stability of EDLCs based on the alternative electrolyte 0.5 M TEABF₄ in EiPS, floating tests at 20, 60, and 80 °C were

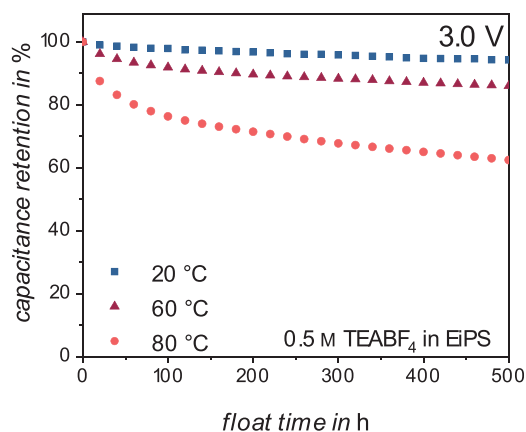


Figure 3. Influence of different temperatures on the floating stability of 0.5 M TEABF₄ in EIPS at 3.0 V.

carried out at the fixed cell voltage of 3.0 V. **Figure 3** shows the comparison of the capacitance retention of the devices after 500 h of floating. As expected, the stability of the devices decreases with increasing temperature. Considering the first hours of floating at temperatures higher than 60 °C, the capacitance decreases relatively fast before the decrease becomes more linear. At the end of the floating time the EDLC operating at 20 °C displays a capacitance retention of 94%, while that of the device operating at 60 °C was 86%. When increasing the temperature further to 80 °C, the aging is accelerated resulting in a decrease of the capacitance retention to 62%. This indicates the presence of more degradation events starting to occur in the temperature range between 60 and 80 °C than in the range between 20 and 60 °C. It is also important to notice that the XRD patterns and XPS spectra of electrodes that were stored for 24 h in the electrolyte solution under the temperatures mentioned (see Figures S3 and S4 in the Supporting Information) show no major changes in the electrode surface and no decomposition of the electrolyte. This is indicated by no major additional crystalline phases emerging in the XRD pattern and minor signals in the XP spectra originating from electrolyte residues which becomes clear when comparing the atomic contents of the heteroatoms in Table S2 in the Supporting Information. Considering these

results, the degradation processes above 60 °C appear to be promoted by the combination of a certain voltage with elevated temperatures and not by an intrinsic instability of the electrolytic solution and/or of the electrodes at this temperature.

To gain further insight into the aging mechanisms of EIPS-based EDLCs, we conducted additional float tests in a modified Swagelok cell designed for post-mortem GC-MS analysis, presented by our group in a previous work.^[8a] In these tests the devices have been floated at 3.0 V at 20, 60, and 80 °C for 100 h. This shortened floating time has been selected to compensate for the reduced performance of the modified cells (which have been discussed in a previous publication). As depicted in **Figure 4a**, also in this case the capacitance retention decreases while the operating temperature is increased. However, in this case, the devices operating at temperatures higher than 60 °C display a strong reduction of capacitance during the initial 5 h of floating. After this initial drop, however, the cells stabilize and show a constant decrease in capacitance till the end of the floating tests. A possible explanation for this behavior could be the formation of a passive layer on the electrode surface at the beginning of the floating test. This passive layer would reduce the capacitance of the electrode material by blocking pores on the surface, while preventing the electrolyte from further decomposition, and therefore increasing the stability of the EDLC afterward. This hypothesis is supported by the evolution of the impedance spectra shown in **Figure 4b**. The spectra clearly show the decrease of the electrolyte resistance at the beginning of the semicircle with increasing temperature, and, more importantly, a significant increase of the charge-transfer resistance in the electrode pores after the initial 5 h of floating, which is represented by the size of the semicircle. This resistance increase corresponds to the initial decrease of capacitance and the possible formation of a passive layer. In order to understand this behavior, we carried out post-mortem GC-MS on the electrolyte and post-mortem XPS of the electrodes.

Figure 5 compares the obtained TICs of the pure EIPS solvent with that of the electrolytes extracted from the EDLCs at the end of the floating test considered above. As shown in **Figure S5** of the Supporting Information, the used solvent shows trace amounts of various impurities. Approximately 14 individual signals have been detected with retention times

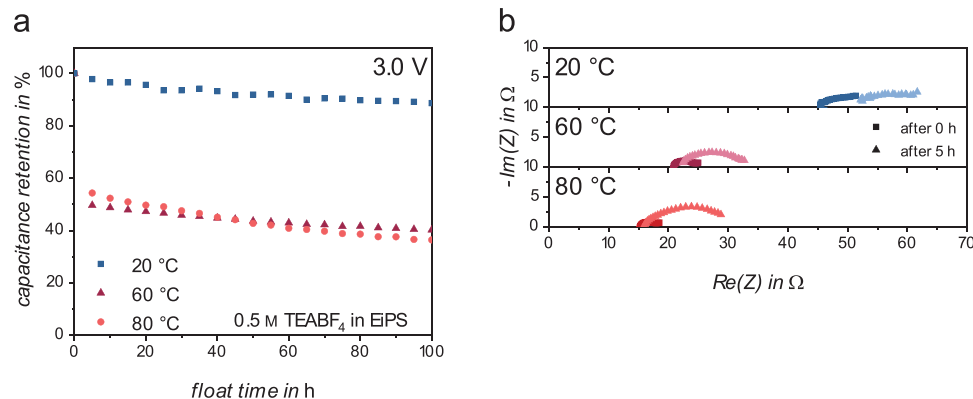


Figure 4. a) Influence of different temperatures on the floating stability and b) comparison of Nyquist plots in the high to mid-frequency range between 500 kHz and 50 Hz before (squares) and after 5 h (triangles) of floating of 0.5 M TEABF₄ in EIPS at 3.0 V in Swagelok cells, modified for post-mortem analysis of the cell components.

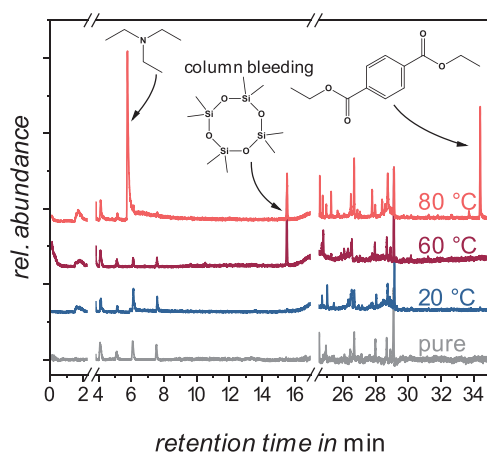
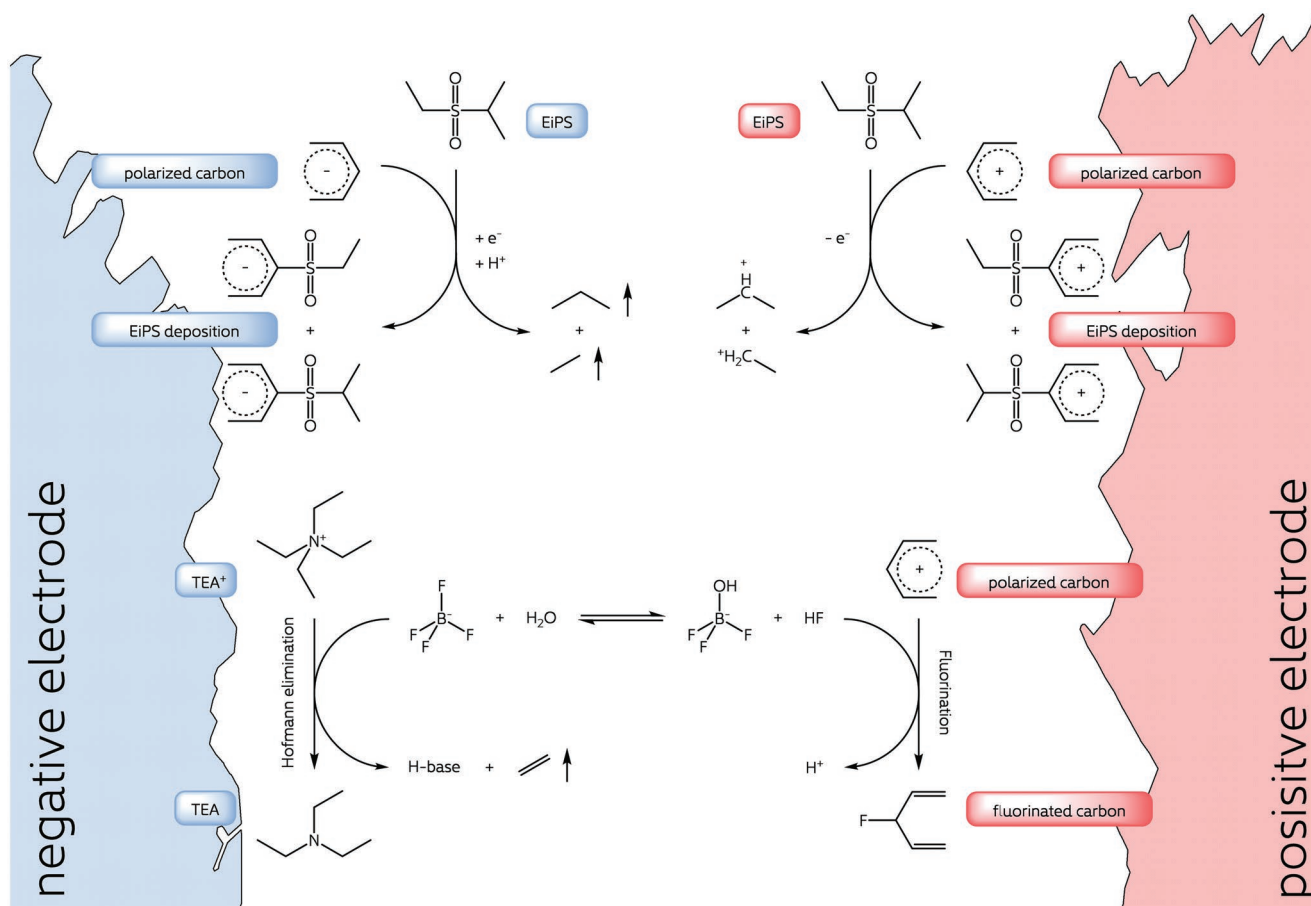


Figure 5. TICs of the post-mortem GC-MS measurements of the aged electrolytes obtained after aging tests of symmetrical EiPS-based EDLCs. The signal has been cropped due to a detector shut-down to prolong the lifetime of the filament during the appearance of the EiPS between 17 and 24.5 min.

between 4 and 8 min and between 24.5 and 29 min and two chemical impurities were identified as diethylsulfolane at 6.1 min and ethyl(isopropyl)sulfolane at 7.55 min. As previously

shown, the presence of various impurities in the base solvent complicates this type of investigation. Nevertheless, additional peaks could be observed on the TICs of the electrolytes extracted from the EDLCs operating at 80 °C. The signal at 15.5 min can be attributed to column bleeding and can thus be neglected for further interpretation. The signals at t_R 6 min and 34 min could be assigned to the formation of triethylamine and diethyl-terephthalate, respectively. The formation of the former compound can be attributed to the decomposition of the cation of the conducting salt (tetraethylammonium), while the one of the latter is due to the degradation of the Mylar-foil which is a component of the cell material consisting of polyethylene terephthalate (PET). The formation of triethylamine, which occurs at 80 °C, is known as a Hofmann elimination, where quaternary amines form tertiary amines and alkenes while a proton is eliminated.^[6a,13] Generally, this is realized by a base such as OH^- , in this case, however, BF_4^- or its hydrolysis product $\text{BF}_3(\text{OH})^-$ can act as such (Scheme 1). Though, ethylene was not detected within the electrolyte. This can be caused by the gaseous state and the outgassing of ethylene from the sample prior to injection and analysis.

Considering the result of the post-mortem GC-MS it is reasonable to suppose that the aging processes occurring in the investigated EiPS-based EDLCs are mainly leading to



Scheme 1. Proposed degradation mechanisms at elevated temperatures of the electrode-electrolyte-interphase in EDLCs based on a solution of TEABF_4 in EiPS and activated carbon electrodes covering the degradation of the electrolyte cation via a Hofmann elimination, the fluorination of the carbon surface, especially by in situ formed HF and the depletion of EiPS decomposition products on the electrode surface.^[11,16]

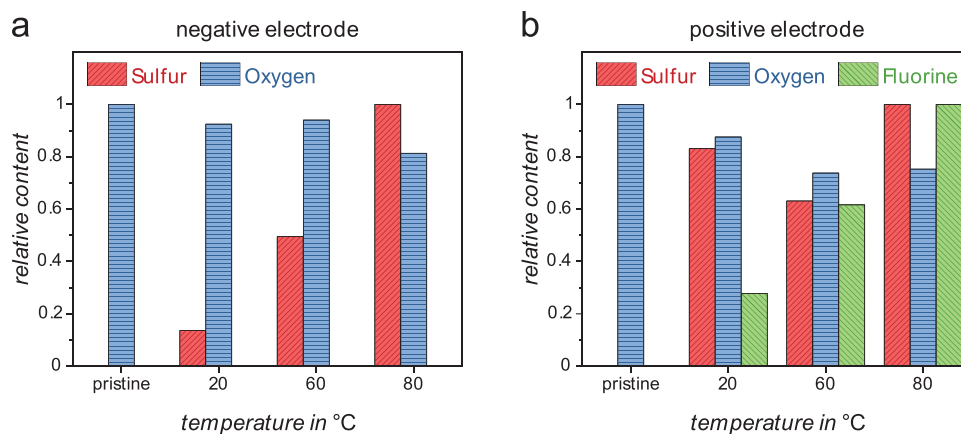


Figure 6. Relative content of sulfur (red), oxygen (blue), and fluorine (green) on the electrode surface after aging tests of symmetrical EIPS-based EDLCs at different temperatures: a) composition of the negative, and b) composition of the positive electrode. The atomic content was normalized with respect to the atomic content of the pristine electrode for oxygen and with respect to the atomic content of the electrodes after aging at 80 °C for sulfur and fluorine, respectively.

the formation of nonsoluble decomposition products, which cannot be detected with this technique. This formation of these products, nonetheless, might lead to pore blocking and/or the formation of a passive layer on the electrode surface. Powder XRD patterns of the electrodes after cycling do not indicate the presence of a passivation layer with pronounced crystallinity (Figure S3 in the Supporting Information), since all observed reflexes (at 38.5°, 45°, 65.5°, and 78.5°) could be assigned to the aluminum current collector. To identify a potential layer formation of noncrystalline compounds, the chemical composition of the electrode surfaces after the floating test, post-mortem XPS measurements have been carried out. Survey spectra of the noncycled electrode as a reference, and the electrochemically aged electrodes at 20, 60, and 80 °C are shown in the supporting information (Figure S6, Supporting Information). The element composition of the electrode surface changes after the aging tests (Figure 6). Compared to the original electrode, the surface of the negative electrode shows an increase in sulfur and a loss of oxygen as indicated additionally by the atomic contents shown in Table S2 in the Supporting Information. Oxygen, which mainly originates from the binder carboxymethyl cellulose (CMC), reacts with sulfur components over time, in particular, with an increase in temperature. Similar observations are made for the surface of the positive electrode. The oxygen content is reduced, while sulfur is increased. Additionally, in the case of the positive electrode, the fluorine content is significantly increased, which points to the deposition of the nucleophilic BF_4^- ions or their decomposition products on the electrode surface.

To further identify reactions of the electrode surface with electrolyte compounds, high-resolution spectra (HR) of sulfur, oxygen, and fluorine were recorded for the electrodes of the EDLCs aged at different temperatures (Figure 7). The O1s, F1s, and S2p HR spectra suggest different deposition mechanisms during the aging process. The original electrode's O1s spectrum shows three different peaks (Figure S7 in the Supporting Information). Those peaks can be assigned to oxygen with a binding environment as in -OH, or ether (533.4 eV), aldehydes and ketones (531.7 eV), and carboxylic O (536.0 eV). All those

functional groups can be assigned to the binder Na-CMC. The aged electrodes mostly exhibit -OH/ether-like oxygen (≈ 533.2 eV). Oxygen as found in carboxylic groups (≈ 536 eV) was removed during electrochemical aging. Changes due to the deposition of sulfoxides cannot be discussed because the binding energy of oxygen in such ($\text{O}=\text{S} \approx 531\text{--}532$ eV) overlaps with those of ether and -OH groups.^[14] The F1s spectra differ for the two electrodes, as well as for the different aging temperatures. The original electrode does not exhibit any fluorine on the surface. TEABF_4 shows one F1s peak at a binding energy of 685.6 eV (Figure S8 in the Supporting Information). This peak is visible in all F1s spectra of the aged electrodes (blue), but more significantly for the positive electrode due to the higher amount of fluorine in total. In addition, aged electrodes show a second F-species at ≈ 687.2 eV, which corresponds to F-species as in polytetrafluoroethylene (PTFE).^[15] In particular, for electrodes aged at 80 °C, this peak becomes the strongest indicating that such F-species are the most dominant occurring F-species on the electrode surface. This fluorination of the carbon surface can be realized especially by HF formed in situ during the hydrolysis of BF_4^- ,^[16] or possibly by the other fluorine-containing species of the hydrolysis equilibrium. Due to the positive surface polarization, this process is more pronounced for the positive electrode leading to a higher total amount of F on the surface (Scheme 1). The buildup of sulfur-containing compounds is related to the deposition of compounds originating from EIPS. Accordingly, the original electrode's XP spectrum does not feature any S-related peaks. After electrochemical aging, S is present on the electrode surface of both electrodes. EIPS, which contains sulfoxidic groups can be found on all electrode surfaces, which is indicated by the doublet peak with its center at ≈ 168.6 eV.^[17] Additionally, a second doublet peak appears with an increase in temperature during aging at a binding energy of ≈ 164.5 eV. Such binding energy can be assigned to sulfur species as in C-S or S-S bonding environments. The formation of such sulfur species is realized through a reduction reaction of sulfoxide. Thus, it is expected that this process is more pronounced on the surface of the negative electrode than on the respective surface of the positive electrode.

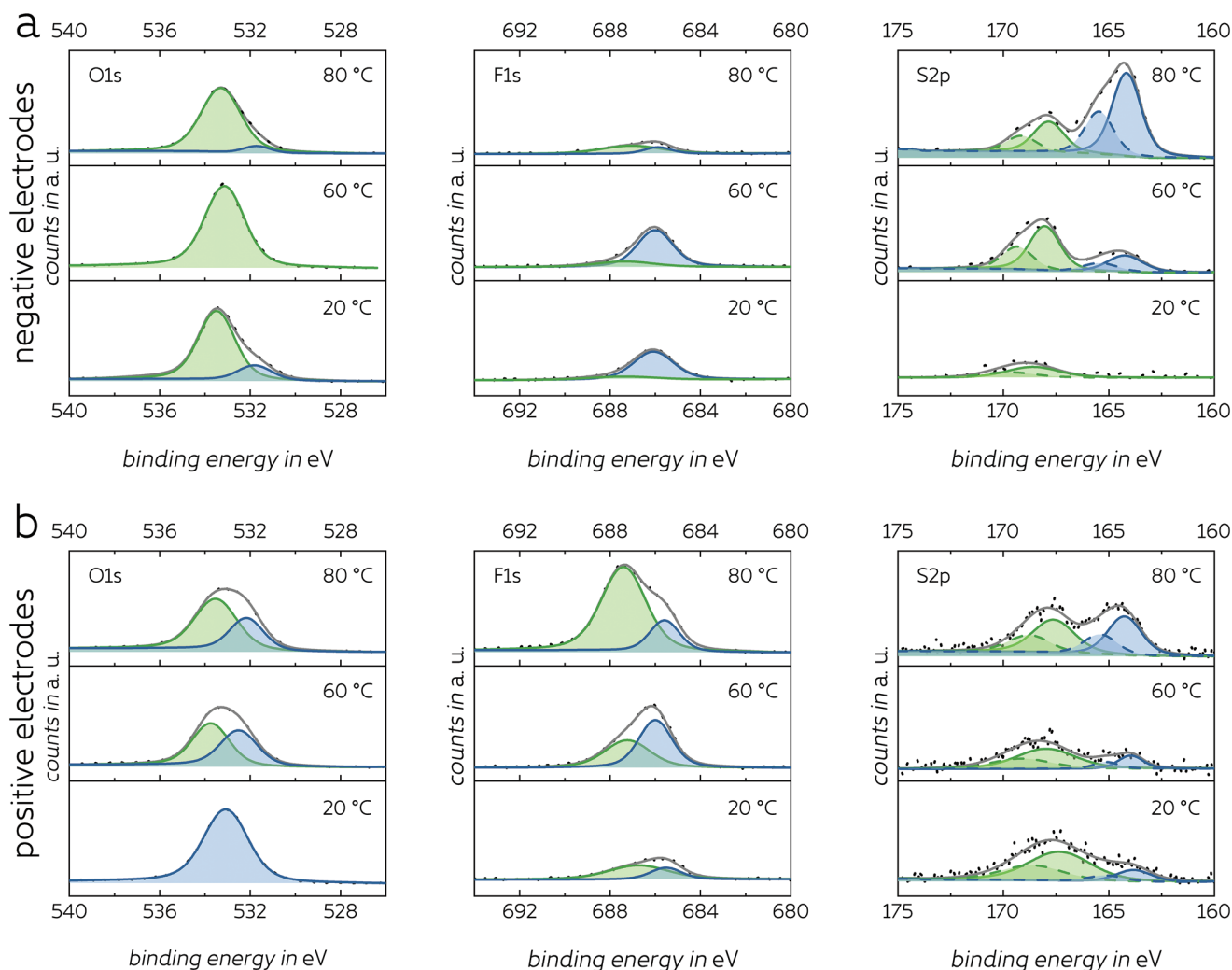


Figure 7. High-resolution XPS spectra of O1s, F1s, and S2p of the a) negative electrodes and b) positive electrodes after electrochemical aging tests of symmetrical EDLCs based on 0.5 M TEABF₄ in EiPS.

These findings, in particular, underline the theory that a passive layer is formed by the deposition of decomposition products of EiPS at increased temperatures. This also correlates well with the electrochemical aging tests (Figure 4). However, the formation of the passivation layer leads to a significant loss of capacitance, while it increases the stability of the system dramatically after its formation.

Based on these findings and decomposition processes already known in the literature, we propose a decomposition mechanism of the electrode-electrolyte-interphase for EDLCs based on activated carbon electrodes and a solution of TEABF₄ in EiPS as electrolyte (Scheme 1). In the presence of water, the hydrolysis of BF₄⁻ into BF₃(OH)⁻ and HF (pK_a H₂O 3.45) takes place, where the balance of the reaction equilibrium is on the left side. Since the acids HBF₄ (pK_a H₂O -0.44) and HBF₃(OH) (slightly weaker than the former) are highly acidic, their corresponding bases are rather weak.^[16,18] However, their presence seems to be sufficient for the elimination reaction being processed at 80 °C. Due to the ion charge, this process is expected to be promoted on the negative electrode. Especially the positive

electrode, on the other hand, shows fluorination of the carbon surface. This can be explained by the in situ formation of HF which can fluorinate the carbon, while it is not clear if the other fluorine-containing species play a role in this fluorination process.^[19] The presence of sulfoxidic groups and C-S bonds on the carbon surface of both electrodes indicates the existence of a reduction as well as an oxidation process with EiPS being involved. The considered reactions were described previously by Chiba et al. and match the experimental results.^[11]

3. Conclusion

In this study, we investigated the use of the electrolyte 0.5 M TEABF₄ in EiPS in EDLCs operating at high voltage and high temperatures. We showed that although this electrolyte displays ionic conductivity and viscosity not as favorable as those of the state-of-the-art electrolyte 1 M TEABF₄ in ACN, it features a very high electrochemical and thermal stability. Thanks to these features, its use allows the realization of EDLCs operating at more

than 3 V at 60 and 80 °C which are much more stable than those containing the state-of-the-art electrolyte. For example, EiPS-based EDLCs are able to retain 75% of their initial capacitance after 500 h of floating at 3.2 V at 60 °C while under these conditions devices containing conventional electrolytes are not stable. Post-mortem GC-MS analysis of the electrolyte revealed no soluble decomposition products originated from the solvent. On the other hand, post-mortem XPS analysis of the electrodes indicated the deposition of nonsoluble decomposition compounds on the electrode surface at temperatures higher than 60 °C. While having a pore blocking and thus capacitance-reducing effect, the layer of decomposition compounds acts as a passivation layer during cell operation after its formation. This increases the electrochemical stability dramatically but, at the same, time, is affecting the capacitance. Considering these results, EiPS can be certainly considered a very interesting electrolyte for the realization of high-voltage EDLCs operating at high temperatures. This could provide a solution for niche applications in high-temperature environments in the future.

4. Experimental Section

Electrolyte Preparation: The solvent EiPS was purchased from TCI Chemicals with a purity of 97%. The initial water content was reduced to 20 ppm by an overpressure Schlenk filtration with predried aluminum oxide under vacuum and additional drying with a molecular sieve with a pore size of 4 Å provided by Chemiewerk Bad Köstritz. The solvent ACN was supplied by Sigma-Aldrich with a purity of 99.8% and dried by the addition of a molecular sieve with a molecular pore size of 3 Å. The salt TEABF₄ was purchased from TCI Chemicals and dried for 24 h in a vacuum glass oven at 120 °C and 1×10^{-2} mbar before use. For the following reported investigations, the electrolytes 0.5 M TEABF₄ in EiPS and 1 M TEABF₄ in ACN were used.

Physicochemical Properties: The ionic conductivity of the electrolytes was measured in a temperature range between -30 and 80 °C with a Modulab XM ECS potentiostat. During the measurements, the conductivity cell was placed in a climatic chamber to adjust the temperature following a procedure as described before.^[20] The viscosity of the electrolytes was measured with an Anton-Paar MCR 102 rotational viscometer applying a shear rate of 1000 s⁻¹ with 500 µL of electrolyte following a procedure identical to a procedure described before.^[20]

Cell Preparation: The utilized composite electrodes for the electrochemical measurements were provided by Skeleton Technologies with an electrode mass loading of 6.8 mg cm⁻². The area of the utilized electrodes was 1.13 cm². The commercial electrodes were coated double-sided with activated carbon as active material. One side of the carbon coating was removed with ethanol before the application to match the experimental setup (as described below).

The electrochemical measurements have been carried out using Swagelok-type cells with a two-electrode setup reference which were mounted in a LABmaster pro glove box by MBRAUN filled with argon with a content of H₂O and O₂ <1 ppm. For the cell setup, two identical electrodes (symmetrical cell) were used with a 520 µm Whatman glass fiber disk as the separator, soaked with 120 µL of electrolyte.

Electrochemical Measurements: The electrochemical stability of the utilized electrolytes was investigated utilizing float tests carried out at different voltages and temperatures for 500 h with an Arbin LBT21084 and a BioLogic VMP-3. During the measurements, the cells were placed in a Binder KB 53 climatic chamber to adjust the temperature. Every 20 h, 5 charge/discharge cycles were performed with a current rate of 1 A g⁻¹ between 0 V and the applied float voltage.

Electrochemical Data Evaluation: The capacitance *C* of the galvanostatic charge-discharge cycles during the float tests was calculated based on

linear extrapolation of the latter 90% of the voltage profile to exclude the initial voltage drop from the extrapolation. Applying the resulting slope $\frac{dV}{dt}$ with the voltage *V* and time *t* to $C = \frac{I}{dV/dt}$ with the applied current *I* leads to the capacitance. The maximum energy *E*_{max} was obtained by integration of the discharge semiperiod of the instantaneous power *p*(*t*):

$$E_{\max} = \int_{t_0}^T p(t) dt = \int_{t_0}^T v(t) i(t) dt \quad (1)$$

with *t*₀ and *T* being the initial and final times of the discharge semiperiod and *v*(*t*) and *i*(*t*) being the instantaneous voltage and current, while the maximum power *P*_{max} equals the maximum of the modulus function of *p*(*t*).

Electrochemical Measurements for Post-Mortem Analysis: To understand the decomposition processes occurring in the investigated systems, float tests with modified Swagelok-type cells were performed with a cell setup as described in a previous publication.^[8a] The cells were filled with 1 mL of electrolyte while a 1 mm thick ring-shaped spacer was utilized. The electrochemical investigation of these modified cells was carried out with a BioLogic VMP-3 and an Arbin LBT21084 by float tests over 100 h at a voltage of 3.0 V and different temperatures. Temperatures were set during the measurement by placing the cells in a Binder KB 53 climatic chamber adjusted to the specific temperature, while every 5 h, 5 charge/discharge cycles were performed between 0 and 3.0 V applying a current rate of 1 A g⁻¹.

Post-Mortem GC-MS Measurements: After 100 h of float test, 300 µL of the electrolyte solution was extracted from the modified Swagelok cells and further analyzed by post-mortem GC-MS measurement. The GC-MS measurements were conducted with an Agilent 7890B GC, equipped with an Agilent 7683 Series automatic liquid sampler (ALS) and an Agilent HP-5ms column (30 m, ID 250 µm, DF 1 µm, -60 – 325 °C), and an Agilent 5977A MS (EI-MSD, single quadrupole). The oven was set to a temperature range of 70–280 °C, heating with a temperature ramp of 10 °C min⁻¹. The injection volume of the sample was set to 5 µL, while a carrier-gas flow (He) of 1 mL min⁻¹ at a split ratio of 3:1 was applied. The resulting mass spectra were evaluated utilizing a NIST/EPA/NIH Mass Spectral Library (version 2.2, build June 10, 2014), with identified analytes showing a match probability of 70% or higher in the total ion chromatograms (TICs). With the obtained TICs, background subtraction and baseline correction were performed.

Post-Mortem XPS Analysis: The electrodes were extracted from the modified Swagelok cells after the electrochemical investigation for post-mortem XPS analysis. The samples for spectroscopy were prepared by cleaning the electrodes in ACN for 24 h followed by drying in a vacuum glass oven at 60 °C and 1×10^{-2} mbar. Subsequently, electrodes were fixated on adhesive copper tape. XP spectra were recorded using a Thermo Scientific KAlpha spectrometer. An Al Kα anode (*hν* = 1486.6 eV) was used as an X-Ray source. The chamber pressure during each measurement was not higher than 5×10^{-8} mbar. A flood gun was used to compensate potential surface charge. Survey scans, which were used to determine the elemental composition, were recorded in a binding energy range of 136.6–1360 eV with a step size of 1 eV and a pass energy of 100 eV. The auto height function was enabled. High-resolution spectra were recorded with a step size of 0.5 eV as 5 averaged scans. Binding energies were referenced to the C1s at 284.8 eV as all samples contain graphitic carbon as a conductive additive. The resulting peak shifting values are given in the supporting information.

Post-Mortem XRD Analysis: X-ray diffraction (XRD) was performed on a Bruker D2 Phaser device using Cu Kα radiation in a 2θ range of 10 – 80° and a step size of 0.02° in Bragg-Brentano geometry, placing the samples on a single-crystal silicon sample holder. The phase assignment was realized using the integrated software module from the crystallography open database.

Supporting Information

Supporting Information is available from the Wiley Online Library or from the author.

Acknowledgements

The authors would like to thank the Friedrich-Schiller-University Jena for their support and L.K., R.G., and A.B. thank the Bundesministerium für Wirtschaft und Klimaschutz (BMWK) within the project "SUPREME" (03EI6060B) for the financial support. M.O. and A.B. acknowledge support by the European Funds for Regional Development (Europäischer Fonds für Regionale Entwicklung; EFRE-OP 2014-2020; Project No. 2021 FGI 0035, NanoLabXPS) as part of the REACT-EU program.

Open access funding enabled and organized by Projekt DEAL.

Conflict of Interest

The authors declare no conflict of interest.

Data Availability Statement

The data that support the findings of this study are available from the corresponding author upon reasonable request.

Keywords

aging, ethyl isopropyl sulfone, high stability, high temperatures, post-mortem analysis, supercapacitors

Received: November 10, 2022

Revised: November 29, 2022

Published online: December 19, 2022

- [1] a) R. Kötz, M. Carlen, *Electrochim. Acta* **2000**, *45*, 2483; b) M. M. Rahman, A. O. Oni, E. Gemechu, A. Kumar, *Energy Convers. Manage.* **2020**, *223*, 113295.
- [2] F. Beguin, V. Presser, A. Balducci, E. Frackowiak, *Adv. Mater.* **2014**, *26*, 2219.
- [3] a) C. Schütter, S. Pohlmann, A. Balducci, *Adv. Energy Mater.* **2019**, *9*, 1900334; b) D. Lasrado, S. Ahankari, K. K. Kar, in *Handbook of Nanocomposite Supercapacitor Materials III*, Vol. 313 (Ed: K. K. Kar), Springer International Publishing, Berlin **2021**, Ch. 10; c) K. V. G. Raghavendra, R. Vinoth, K. Zeb, C. V. V. Muralee Gopi, S. Sambasivam, M. R. Kummara, I. M. Obaidat, H. J. Kim, *J. Energy Storage* **2020**, *31*, 101652.
- [4] a) Z. Lin, E. Goikolea, A. Balducci, K. Naoi, P. L. Taberna, M. Salanne, G. Yushin, P. Simon, *Mater. Today* **2018**, *21*, 419; b) J. R. Miller, P. Simon, *Science* **2008**, *321*, 651; c) T. P. Sumangala, M. S. Sreekanth, A. Rahaman, in *Handbook of Nanocomposite Supercapacitor Materials III*, Vol. 313 (Ed: K. K. Kar), Springer International Publishing, Berlin **2021**, Ch. 11; d) J. Y. Zhao, A. F. Burke, *J. Energy Chem.* **2021**, *59*, 276.
- [5] a) R. Carter, A. Cruden, P. J. Hall, *IEEE Trans. Veh. Technol.* **2012**, *61*, 1526; b) L. Kouchachvili, W. Yaïci, E. Entchev, *J. Power Sources* **2018**, *374*, 237; c) R. T. Meyer, R. A. Decarlo, S. Pekarek, *Asian J. Control* **2016**, *18*, 150; d) Z. Song, J. Li, J. Hou, H. Hofmann, M. Ouyang, J. Du, *Energy* **2018**, *154*, 433.
- [6] a) P. Kurzweil, M. Chwistek, *J. Power Sources* **2008**, *176*, 555; b) P. Kurzweil, J. Schottenbauer, C. Schell, *J. Energy Storage* **2021**, *35*, 102311.
- [7] J. Krummacher, C. Schütter, L. H. Hess, A. Balducci, *Curr. Opin. Electrochem.* **2018**, *9*, 64.
- [8] a) L. Köps, F. A. Kreth, A. Bothe, A. Balducci, *Energy Storage Mater.* **2022**, *44*, 66; b) A. Brandt, A. Balducci, *J. Power Sources* **2014**, *250*, 343.
- [9] a) A. Balducci, *J. Power Sources* **2016**, *326*, 534; b) A. Brandt, S. Pohlmann, A. Varzi, A. Balducci, S. Passerini, *MRS Bull.* **2013**, *38*, 554; c) L. H. Hess, A. Balducci, *Electrochim. Acta* **2018**, *281*, 437; d) A. Krause, A. Balducci, *Electrochim. Commun.* **2011**, *13*, 814; e) M. Schoeder, P. Isken, M. Winter, S. Passerini, A. Lex-Balducci, A. Balducci, *J. Electrochem. Soc.* **2013**, *130*, A1753; f) T. Stettner, A. Balducci, *Energy Storage Mater.* **2021**, *40*, 402.
- [10] a) A. Bothe, A. Balducci, *Electrochim. Acta* **2021**, *374*, 137919; b) A. Bothe, A. Balducci, *J. Power Sources* **2022**, *548*, 232090; c) M. Hahn, R. Kötz, R. Gallay, A. Siggel, *Electrochim. Acta* **2006**, *52*, 1709; d) R. Kötz, P. W. Ruch, D. Cericola, *J. Power Sources* **2010**, *195*, 923; e) L. H. Hess, A. Bothe, A. Balducci, *Energy Technol.* **2021**, *9*, 2100329.
- [11] K. Chiba, T. Ueda, Y. Yamaguchi, Y. Oki, F. Shimodate, K. Naoi, *J. Electrochem. Soc.* **2011**, *158*, A872.
- [12] C. Schütter, A. Bothe, A. Balducci, *Electrochim. Acta* **2020**, *331*, 135421.
- [13] K. Schwetlick, *Organikum*, Wiley-VCH, Weinheim, Germany **2015**.
- [14] a) T. G. Avval, C. V. Cushman, S. Bahr, P. Dietrich, M. Meyer, A. Thißen, M. R. Linford, *Surf. Sci. Spectra* **2019**, *26*, 014020; b) C. Schneidermann, C. Kensy, P. Otto, S. Oswald, L. Giebeler, D. Leistenschneider, S. Grätz, S. Dörfler, S. Kaskel, L. Borchardt, *ChemSusChem* **2019**, *12*, 310.
- [15] T. A. Blanchet, F. E. Kennedy, D. T. Jayne, *Tribol. Trans.* **1993**, *36*, 535.
- [16] A. F. Hollemann, E. Wiberg, N. Wiberg, *Lehrbuch der Anorganischen Chemie*, Walter de Gruyter, Berlin **2007**.
- [17] P. Louette, F. Bodino, J.-J. Pireaux, *Surf. Sci. Spectra* **2005**, *12*, 100.
- [18] D. R. MacFarlane, S. A. Forsyth, in *Ionic Liquids as Green Solvents*, Vol. 856 (Eds: R. D. Rogers, K. R. Seddon), American Chemical Society, NY **2003**, Ch. 22.
- [19] Y. Liu, L. Jiang, H. Wang, H. Wang, W. Jiao, G. Chen, P. Zhang, D. Hui, X. Jian, *Nanotechnol. Rev.* **2019**, *8*, 573.
- [20] L. H. Hess, A. Balducci, *ChemSusChem* **2018**, *11*, 1919.